Polymeric architectures of bismuth citrate based on dimeric building blocks

YANG Nan[1], AN Yan[2,3], CAI JiWen[4], HU LiHong[1], ZENG YiBo[1], MAO ZongWan[2], CHEN GuanHua[1] & SUN HongZhe[1*]

[1]*Department of Chemistry, The University of Hong Kong, Hong Kong, China*
[2]*School of Chemistry and Chemical Engineering, Sun Yat-Sen University, Guangzhou 510275, China*
[3]*Institute of Marine Materials Science and Engineering, Shanghai Maritime University, Shanghai 201306, China*
[4]*School of Pharmaceutical Sciences, Sun Yat-Sen University, Guangzhou 510080, China*

Four bismuth complexes, $(H_2En)[Bi_2(cit)_2(H_2O)_{4/3}] \cdot (H_2O)_x$ (**1**), $(H_2En)_3[Bi_2(cit)_2Cl_4] \cdot (H_2O)_x$ (**2**), $(HPy)_2[Bi_2(cit)_2(H_2O)_{8/5}] \cdot (H_2O)_x$ (**3**) and $(H_2En)[Bi_2(cit)_2](H_2O)_x$ (**4**) [cit = citrate^{4-}; En = ethylenediamine; Py = pyridine] have been synthesized and crystallized. The crystal structures reveal that the basic building blocks in all of these complexes are bismuth citrate dimeric units which combine to form polymeric architectures. The embedded protonated ethylenediamine and pyridine moieties in the polymeric frameworks have been identified by X-ray crystallography and solid-state cross polarization/magic angle spinning (CP/MAS) ^{13}C NMR. Based on the framework of complex **1**, a structural model of a clinically used antiulcer drug, ranitidine bismuth citrate (RBC) was generated. The behavior of the protonated amine-bismuth citrate complexes in acidic aqueous solution has been studied by electrospray ionization-mass spectrometry (ESI-MS).

bismuth citrate, polymeric architecture, crystal structure, solid-state NMR, ESI-MS

1 Introduction

Heavy metals are notorious for their toxicity. However, the medical use of the heaviest stable element, bismuth—which utilizes its antimicrobial activity and low collateral toxicity—can be traced back to the Middle Ages. Based on our increasing knowledge of the characteristics of bismuth, many of its compounds have been synthesized and used in human healthcare[1–3]. In particular, bismuth citrate-based (Bi(cit)-based) compounds have been clinically used worldwide to treat peptic ulcers and exhibit promising antiviral activities[4–6]. Two Bi(cit)-based drugs, colloidal bismuth subcitrate (CBS, De-Nol® and Lizhudele®) and ranitidine bismuth citrate (RBC, Tritec® and Pylorid®), when used in combination with antibodies, show the highest therapeutic

efficiency for *Helicobacter pylori* (*H. pylori*) infection[7].

Due to the importance of CBS and RBC, enormous efforts have been made to elucidate their structures. However, the structures of bismuth citrate-based complexes are complicated due to their tendency to polymerize. The empirical formula of CBS was previously given as $K_3(NH_4)_2[Bi_6O_3(OH)_5(Hcit)_4]$, but has been changed to "polymeric bismuth citrate complex" in the latest edition of the Merck Index to reflect its complicated polymeric features[8]. Nine bismuth citrate adducts have been structurally characterized by X-ray crystallography and NMR spectroscopy[9–12]. Most of them are composed of stable bismuth citrate dimeric units $([Bi(cit)_2Bi]^{2-})$ and additional O^{2-}, OH^- or H_2O ligands. It is believed that the $[Bi(cit)_2Bi]^{2-}$ unit forms negatively charged polymeric skeletons in bismuth citrate complexes and aggregates giving a type of "hybrid" metal-organic framework (MOF)[9–13]. However, most reports of the structures of bismuth citrate complexes are based on their crys-

tals obtained at neutral pH, which may fail to reflect the structural features of Bi(cit)-based complexes when used as drugs, since Bi(cit)-based drugs are designed for treating diseases in the stomach where the physiological acidity is close to pH 3. The crystal structures of Bi(cit)-based complexes at low pH, therefore, can more precisely reflect their structural features under actual therapeutic conditions.

In order to study the polymeric properties and degradation pathways of bismuth citrate complexes, we report here the structures of four Bi(cit)-based complexes that are formed via the assembly of bismuth citrate dimeric units ($[Bi(cit)_2Bi]^{2-}$) with various amines under acidic conditions. The thermal degradation behavior of these amine-Bi(cit)-based complexes and a structural model of RBC based on the framework of one such complex are also reported herein.

2 Experimental

2.1 Materials

Bismuth citrate, ethylenediamine (En), pyridine (Py) and ranitidine (Ran) were all obtained from Sigma-Aldrich and used directly without further purification.

2.2 Solid-state ^{13}C NMR spectra

Solid-state ^{13}C NMR spectra were recorded on a Varian InfinityPlus-400 spectrometer equipped with a Chemagnetic 2.5 mm double resonance probe at 100.4 MHz, using cross polarization/magic angle spinning (CP/MAS). Spinning speeds of 8 kHz with a 5 ms contact time were used. Spatially selective composite pulses were combined with conventional CP pulse sequences in order to effectively suppress weak signals (background) from the spinning module.

2.3 Single crystal X-ray crystallography

The structures of tiny crystals of complexes **1**, **2**, **3** and **4** (with crystal sizes of 0.10 mm × 0.05 mm × 0.03 mm, 0.10 mm × 0.05 mm × 0.05 mm, 0.10 mm × 0.08 mm × 0.08 mm and 0.08 mm × 0.05 mm × 0.03 mm respectively) were solved using an Oxford Diffraction Xcalibur Nova single crystal diffractometer with Cu radiation at 120 K. The crystal data and details of the refinement are summarized in Table S1 in the Supporting Information.

2.4 Structure modeling of ranitidine bismuth citrate

Relevant bismuth parameters in the Dreiding force field were generated by the strategy proposed in Universal Force Field (UFF). The parameters were set as follows: the harmonic bond length of Bi–O was set at 2.175 Å with sp^3 hybridized oxygen atoms, the natural bond angle was set at 90°, and the van der Waals radius of bismuth was taken as 4.37 Å with a well depth of 0.518 kcal/mol. Docking of ranitidine into channels formed in bismuth citrate was performed by LigandFit adopted in *Cerius2* with the Dreiding force field.

### 2.5 Electrospray ionization-mass spectrometry

Samples of amine-Bi(cit) complexes for ESI-MS were prepared by dissolving a suspension of bismuth subcitrate (*ca.* 0.2 g) in different diluted amine solutions such as ammonia, ethylenediamine, pyridine and ranitidine. The pH values of the solutions were gradually adjusted to 3.0 by addition of dilute HCl and they were then allowed to stand overnight. After filtration, the pH values of the filtrates were adjusted to *ca.* 4.5 for ESI-MS experiments.

ESI-MS experiments were performed on a LCQ spectrometer (Finnigan Corp, San Jose, CA, USA). The samples were infused at 5 μL/min, and the ions were produced in an atmospheric pressure ionization/ESI ion source. The source temperature was 200 °C with a sheath gas flow rate of 0.9 L/min. A potential of 4 kV was applied to the probe tip, and a cone voltage of 5–10 V was used over the range 200–2000 Da.

3 Results and discussion

3.1 Synthesis

Bi(cit)-based complexes $(H_2En)[Bi_2(cit)_2(H_2O)_{4/3}]\cdot(H_2O)_x$ $(H_2En = [H_3NCH_2CH_2NH_3]^{2+}$, cit $= [C_6H_4O_7]^{4-})$ (**1**), $(H_2En)_3[Bi_2(cit)_2Cl_4]\cdot(H_2O)_x$ (**2**), $(HPy)_2[Bi_2(cit)_2(H_2O)_{8/5}]\cdot$ $(H_2O)_x$ $(HPy = [C_5H_6N]^+)$ (**3**) and $(H_2En)[Bi_2(cit)_2](H_2O)_x$ (**4**) were prepared and crystallized by a similar route to that reported for the complex $K(NH_4)[Bi_2(cit)_2(H_2O)_2]\cdot4H_2O^{[14]}$. The synthesis routes and general crystal data for complexes **1**, **2**, **3** and **4** are summarized in Scheme 1 and Table S1 in the Supporting Information, respectively. After addition of
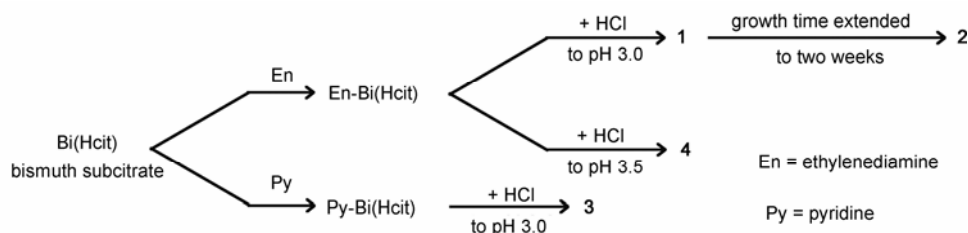
Scheme 1 Synthesis of the bismuth citrate-based complexes **1**, **2**, **3** and **4**.

dilute HCl to a solution of ethylenediamine and bismuth subcitrate, a white precipitate formed and was removed by filtration. Upon standing the filtrate (pH ~3) at room temperature overnight, colorless crystals of **1**, suitable for X-ray analysis, were formed. Crystals of **2** were obtained from the same mother liquor as for **1** on further standing for 1-2 weeks. Colorless crystals of **3**, suitable for X-ray analysis, were obtained in a similar fashion using pyridine to dissolve the bismuth subcitrate. Complex **4** was synthesized by the same route as **1** when the mixture was allowed to crystallize at pH 3.5.

3.2   Crystal structures

Three types of bismuth citrate dimers ($[Bi(cit)_2Bi]^{2-}$) are found in the crystal structure of **1**. The ligands that coordinate to bismuth and the coordination bond lengths in different types of $[Bi(cit)_2Bi]^{2-}$ are summarized in Table S2 in the Supporting Information. Dimers I and II linearly aggregate along the *c* axis to form infinite polyanions that are concomitantly linked by dimer III to generate two-dimensional (2-D) polymeric sheets in the *ac* plane. The aggregation of dimer III along the *b* axis links these 2-D polymeric sheets, resulting in a three-dimensional (3-D) polymeric framework (Figure 1(b)). Surprisingly, no ethylenediamine moieties can be identified by X-ray crystallography. However, the solid-state CP/MAS ^{13}C NMR spectrum of **1** shows a very strong peak at 37.9 ppm, which can be assigned to the carbon atoms of ethylenediamine. The presence of just a single peak indicates that the ethylenediamine moieties are embedded and disordered in the bismuth citrate channels. Other peaks between 43 and 190 ppm can be assigned to the six carbon atoms of bound citrate ligands (Figure 2)[14, 15].

The structure of complex **2** is composed of a unique $[Bi(cit)_2Bi]^{2-}$ dimer. Chloride ligands bridge two adjacent dimers, resulting in infinite polymeric sheets in the *bc* plane

Figure 1   (a) The bismuth citrate dimeric building block ($[Bi(cit)_2Bi]^{2-}$) present in complexes **1–4**; (b) the polymeric framework of **1** (dimers I, II and III are represented by adjacent green, blue and purple polyhedra, respectively); (c) the 2-D polymeric structure of **2** (dimeric units are represented by adjacent green polyhedra) with ethylenediamine skeletons represented in the ball and stick mode; (d) the polymeric framework of **3** (dimers I, II, III, IV and V are represented by adjacent green, blue, red, yellow and purple polyhedra, respectively) with pyridine rings also shown in the space-filling mode; (e) the polymeric framework of **4** (dimeric units are represented by adjacent light blue polyhedra). Color code: C, grey; Bi, yellow; O, red; Cl, green; N, blue. Hydrogen atoms and non-coordinated water molecules are omitted for clarity.
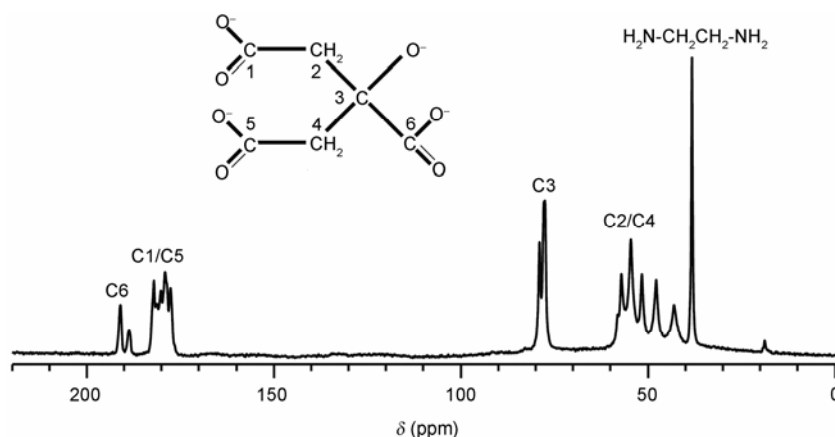
Figure 2 Solid-state CP/MAS ^{13}C NMR spectrum of complex **1**. The assignments together with the structure of the citrate tetraanion ($[C_6H_4O_7]^{4-}$) are shown. The peaks between 175 and 190 ppm can be assigned to the terminal carboxylate carbon atoms (C1/C5), and the two peaks at ~78.6 ppm and the six peaks at 43-57 ppm can be assigned to the central carbon (C3) and C2/C4, respectively. A strong single peak at 37.9 ppm can be assigned to the carbon atoms of disordered ethylenediamine in the framework.

(Figure 1(c)). There are no covalent crosslinks between the adjacent polymeric sheets except for hydrogen bonds (H-bonds) and other electrostatic interactions, suggesting that complex **2** adopts a 2-D structure.

Five different types of $[Bi(cit)_2Bi]^{2-}$ dimers are observed in the structure of complex **3**. An infinite linear polyanion is formed by the aggregation of dimers I and II along the *c* axis. Adjacent polyanions are then connected by dimer IV to form 2-D polymeric sheets in the *bc* plane. The concomitant crosslinking of dimer II with dimer III and dimer IV with dimer V along the *a* axis leads to a 3-D framework. Pyridine moieties are observed clearly in the cavities (Figure 1(d)).

Only one type of $[Bi(cit)_2Bi]^{2-}$ anion is observed in complex **4**. Two deprotonated hydroxyl groups of the citrate ligand connect the adjacent dimeric units. However, in contrast to **2**—which adopts a 2D architecture—the adjacent dimeric units in **4** are crosslinked by coordination bonds along the *a* and *b* axes to form polymeric sheets in the *ab* plane and concomitantly build up a 3-D framework via assembly along the *c* axis (Figure 1(e)). No ethylenediamine could be identified in the crystal structure. However, elemental analysis showed the presence of ethylenediamine in the complex. In the solid-state CP/MAS ^{13}C NMR spectrum of **4**, two peaks at 35.2 and 38.6 ppm were observed, confirming the presence of ethylenediamine embedded in the framework of **4** (Figure S1 in the Supporting Information).

All the citrate anions in the structures of complexes **1–4** are fully deprotonated giving citrate tetraanions ($[C_6H_4O_7]^{4-}$). When two citrate tetraanions coordinate with two Bi^{3+} cations, the excess negative charges in these polyanionic frameworks are balanced by $[H_3NCH_2CH_2NH_3]^{2+}$ or $[C_5H_6N]^+$ cations. The common structural feature suggests that low-molecular mass molecules or ions can be encapsulated by either a diffusion process or electrostatic interactions, similar to the "uptake process" of cations or small molecules by zeolites. However, the size and level of protonatation of the inserted cations also affect the assembly of bismuth citrate dimers. As shown in Figure S2 in the Supporting Information, different shapes of channels and cavities are formed in the frameworks of **1** and **3** due to the use of different type of cations. The cations fill up the cavities formed in the bismuth citrate skeletons to achieve charge balance. Acidity is another key factor that affects the architecture of bismuth citrate complexes. Using the same cation ($[H_3NCH_2CH_2NH_3]^{2+}$) but crystallizing at different pH, two different types of frameworks were obtained, namely complexes **1** and **4**. Growth time is also an important factor. Conversion of complex **1** into **2** was observed when the crystal growth time was extended, indicating that **2** is a more thermodynamically stable form than **1**. When the bridging citrate anions that link the adjacent polymeric sheets in **1** are substituted by Cl$^-$, the complex loses the polymeric linkers in one direction which results in the breakup of the 3-D framework. Such a degradation process may be of relevance as far as the pharmacokinetic behavior of bismuth citrate-based drugs in the stomach is concerned.

3.3 Thermal decomposition studies

The thermogravimetric-differential thermogravimetric (TG-DTG) traces of complexes **1**, **3** and **4** are shown in Figure S3 in the Supporting Information. The observation of peaks below 200 °C in the DTG curves of complexes **1**, **3** and **4**, together with the accompanying weight losses in the TG curves, indicates that small molecules (e.g. water) are released from the bismuth citrate frameworks. Complexes **1**, **3** and **4** lose *ca.* 10%, 20% and 8% of their weight below 200 °C, respectively, indicative of their relative encapsulation capacities.

Figure 3 Structural model of ranitidine bismuth citrate with ranitidine inserted, based on the framework of **1** (ranitidine is represented in the space-filling mode with the carbon atoms highlighted in green). Note that the surface is modeled with the use of solvent-molecule interactions (probe interaction of 1.4 Å). Non-coordinated water molecules are omitted for clarity. Color code: C, dark grey; H, white; O, red; N, blue; S, orange.

3.4 Structural model of ranitidine bismuth citrate

Since previous experiments have demonstrated that a bismuth citrate polymeric skeleton is present in RBC[15], a structural model of RBC based on the framework of **1** was constructed[16]. As shown in Figure 3, ranitidine molecules can be readily embedded into the cavities perpendicular to the *bc* plane. H-bonds are probably formed between ranitidine molecules and the bound citrate ligands. N1 and N2 of ranitidine form N-H⋯O bonds with the citrate in dimer I with H⋯O distances of 2.814 (N1) and 2.524 (N2) Å respectively; in addition the sulfur atom of ranitidine forms a H-bond with a water molecule that coordinates to Bi^{3+} in dimer I with an S⋯H distance of 2.132 Å.

3.5 ESI-MS of amine-bismuth citrate complexes

ESI-MS and tandem mass spectrometry (MS/MS) have recently been successfully used to provide definitive assignments for fragments and molecular species of bismuth compounds in aqueous solutions[17], since the chemical ionization process is mild and does not lead to significant fragmentation, and ions present in solution can be transferred directly into the source[18,19]. To study the behavior of Bi(cit)-based complexes in aqueous solution, samples of bismuth citrate dissolved in different amines were prepared. Their ESI-MS and MS/MS data were then recorded after incubation at pH 3.0 (Figure S4 in the Supporting Information).

In the ESI-MS spectra of ammonia-Bi(cit) (NH₃-Bi(cit)) and pyridine-Bi(cit) (Py-Bi(cit)), peaks ([M]⁺) at *m/z* of 1592.4(±0.2), 1194.6(±0.1) and 796.8(±0.1) were observed and can be assigned to the bismuth citrate tetramer ([Bi₄(cit)₄·5H]⁺, $C_{24}H_{21}O_{28}Bi_4$, *calcd.*, 1592.94), trimer ([Bi₃(cit)₃·4H]⁺, $C_{18}H_{16}O_{21}Bi_3$, *calcd.*, 1194.86) and dimer ([Bi₂(cit)₂·3H]⁺, $C_{12}H_{11}O_{14}Bi_2$, *calcd.*, 796.98), respectively (Table 1). Although no peak at *m/z* of 796.98 is observed in the spectrum of ethylenediamine-Bi(cit) (En-Bi(cit)), a peak at a *m/z* of 856.9 was present, and the MS/MS of this peak showed a peak at *m/z* of 796.7, corresponding to the loss of ethylenediamine from a bismuth citrate dimeric species [Bi₂(cit)₂(En)·3H]⁺ ($C_{14}H_{19}O_{14}N_2Bi_2$, *calcd.*, 857.04) (Table

1). Similar behavior was also observed for Py-Bi(cit), i.e. the MS/MS for *m/z* of 875.7 showed a peak at *m/z* of 796.7, corresponding to the loss of pyridine from a dimeric species [Bi₂(cit)₂(Py)·3H]⁺ ($C_{17}H_{16}O_{14}NBi_2$, *calcd.*, 876.03) (Table 1). No spectrum of ranitidine-Bi(cit) (Ran-Bi(cit)) could be obtained, probably due to the facile ionization of ranitidine molecules which suppresses the signal intensity of bismuth citrate; however, peaks corresponding to bismuth citrate trimer and dimer were still observed.

Although the ESI-MS results give a qualitative reflection of the nature of the bismuth citrate species in solution, quantitative analysis is inappropriate, as the ion signal reflects the extent of chemical ionization as well as relative abundance. If each bismuth citrate species in the series is assumed to be protonated at the same type of site, a semi-quantitative correlation between the abundance and signal intensity is expected. It is certain that low molecular weight bismuth citrate species (dimers) have a higher abundance than that of high molecular weight species (trimers, tetramers). The observation of bismuth citrate oligomers corresponding to tetramers (*m/z* 1592.5), trimers (*m/z* 1194.6) and dimers (*m/z* 796.8) together with gradually increasing abundance indicates that the Bi(cit)-based poly-

Table 1 ESI-MS and MS/MS data for bismuth citrate-based complexes

Complex	*m/z* (+ve)	Assignment (+ve)	MS/MS	Neutral
NH₃-Bi(cit)	796.8 (80)	[Bi₂(cit)₂·3H]⁺		
	1194.6 (43)	[Bi₃(cit)₃·4H]⁺		
	1592.5 (20)	[Bi₄(cit)₄·5H]⁺		
Enᵃ⁾-Bi(cit)	856.9 (100)	[Bi₂(cit)₂(En)·3H]⁺	796.7	En
	1194.6 (33)	[Bi₃(cit)₃·4H]⁺		
Pyᵇ⁾-Bi(cit)	796.7 (100)	[Bi₂(cit)₂·3H]⁺	796.7	Py
	875.7 (54)	[Bi₂(cit)₂(Py)·3H]⁺		
	1194.5 (73)	[Bi₃(cit)₃·4H]⁺		
	1592.3 (30)	[Bi₄(cit)₄·5H]⁺		
Ranᶜ⁾-Bi(cit)	315.1 (46)	Ran		
	796.8 (54)	[Bi₂(cit)₂·3H]⁺		
	905.1 (10)	[Bi(cit)₂(Ran)·6H]		
	1194.5 (23)	[Bi₃(cit)₃·4H]⁺		

a) En = ethylenediamine; b) Py = pyridine; c) Ran = ranitidine.

mers degrade from high molecular weight polymeric species to low molecular weight species (e.g. dimeric units) in solution. In contrast, no such series of degradation peaks is observed for amine-Bi(cit) in the absence of incubation at acidic pH, suggesting that acid plays an essential role in the decomposition of Bi(cit)-based complexes.

4 Conclusion

X-ray crystal structures of four bismuth citrate-based complexes (**1**, **2**, **3** and **4**) reveal that bismuth citrate dimeric units serve as their basic building blocks, leading to all the complexes having polymeric structures with regular meshes and internal cavities. The composition of the complex frameworks depends on the size and level of protonation of the cation, the pH and time of crystallization. The degradation of **1** into **2** may be reflected in the pharmacokinetic behavior of bismuth citrate-based drugs. The polymeric meshes and cavities of complexes **1**, **3** and **4** are responsible for their abilities to encapsulate small molecules, as demonstrated by single crystal X-ray diffraction, solid-state NMR, and TG-DTG. Based on the framework of **1**, a structural model of RBC, the latest bismuth citrate anti-ulcer drug, has been constructed, showing how ranitidine molecules insert into polymeric channels inside the bismuth citrate framework. ESI-MS studies of the amine-bismuth citrate in acidic solutions depict a possible degradation pathway for the bismuth citrate skeleton in gastric acid (pH ~3), i.e. Bi(cit)-based drugs may deposit as a polymer on ulcer craters, then degrade into low molecular weight species either by the action of gastric acid or chloride/water and finally be fully decomposed into basic units such as $[Bi(cit)_2Bi]^{2-}$ that can be subsequently absorbed by either a membrane receptor such as FecA[20] or transported via iron transport pathways[21]. Based on our studies, we propose a possible pharmacokinetic pathway for bismuth citrate-based drugs involving the degradation of the bismuth citrate skeleton from a 3-D polymeric framework to 2-D polymeric sheets and finally to basic dimeric units under acidic conditions. Such a process at low pH may allow the "encapsulated" drugs (e.g. ranitidine) to be released from the porous bismuth citrate matrix. Moreover, the low toxicity and negatively charged frameworks with regular mesh structure suggest that bismuth citrate-based polymers may be a new type of "hybrid" metal-organic framework (MOF) with other potential applications, e.g. as a drug carrier.

1   Stavila V, davidovich RL, Gulea A, Whitmire KH. Bismuth(III) complexes with aminopolycarboxylate and polyaminopolycarboxylate ligands: chemistry and structure. *Coord Chem Rev*, 2006, 250: 2782–2810

2   Sadler PJ, Li H, Sun H. Coordination chemistry of metals in medicine: Target sites for bismuth. *Coord Chem Rev*, 1999, 185–186: 689–709

3   (a) Yang N, Tanner JA, Zheng BJ, Watt RM, He ML, Lu LY, Jiang JQ, Shum KT, Lin YP, Wong KL, Lin MCM, Kung HF, Sun H, Huang JD. Bismuth complexes inhibit the SARS coronavirus. *Angew Chem Int Ed*, 2007, 46: 6464–6468 (b) Yang N, Tanner JA, Wang Z, Huang JD, Zheng BJ, Zhu N, Sun H. Inhibition of SARS coronavirus helicase by bismuth complexes. *Chem Commun*, 2007, 4413–4415

4   (a) Suerbaum S, Michetti P. Medical progress: *Helicobacter pylori* infection. *New Engl J Med*, 2002, 347: 1175–1186 (b) Gisbert JP, Gonzalez L, Calvet X. Systematic review and meta-analysis: Proton pump inhibitor vs. ranitidine bismuth citrate plus two antibiotics in *Helicobacter pylori* eradication. *Helicobacter*, 2005, 10: 157–171 (c) Marshall B. Helicobacter connections. *ChemMedChem*, 2006, 1: 783–802

5   (a) Kamberoglou D, Polymeros D, Sanidas I, Doulgeroglou V, Savva S, Patra E, Tzias V. Comparison of 1-week vs. 2- or 4-week therapy regimens with ranitidine bismuth citrate plus two antibiotics for *Helicobacter pylori* eradication. *Aliment Pharmacol Ther*, 2001, 15: 1493–1497 (b) Yang N, Sun H. Biocoordination chemistry of bismuth: Recent advances. *Coord Chem Rev*, 2007, 251: 2354–2366

6   (a) Briand GG, Burford N. Bismuth compounds and preparations with biological or medicinal relevance. *Chem Rev*, 1999, 99: 2601–2657 (b) Thompson KH, Orvig C. Boon and bane of metal ions in medicine. *Science*, 2003, 300: 936–939 (c) Sun H, Zhang L, Szeto K Y. Inhibition of alcohol dehydrogenase by bismuth. *Met Ions Biol Syst*, 2004, 41: 333–378

7   Beales ILP. Efficacy of *Helicobacter pylori* eradication therapies: a single centre observational study. *BMC Gastroenterology*, 2001, 1: 7–15

8   Merck Index, 14th ed. Merck, Whitehouse, NJ, USA, 2006

9   Asato E, Driessen WL, De Graaff RAG, Hulsbergen FB, Reedijk J. Synthesis, structure, and spectroscopic properties of bismuth citrate compounds. 1. crystal structures of $K_{5-x}(NH4)_x[Bi_2(cit)_2(Hcit)](H_2O)_y$ ($x = 0.25$, $y = 13$) and $(NH_4)_8[Bi_2(cit)_2(Hcit)_2(H_2O)_4](H_2O)_2$. *Inorg Chem*, 1991, 30: 4210–4218

10   Asato E, Katsura K, Mikuriya M, Fujii T, Reedijk J. Isolation of a unique hexanuclear $[Bi_6O_4OH(cit)_3(H_2O)_3]^{3-}$ cluster from the bismuth-containing ulcer healing agent "colloidal bismuth subcitrate (CBS)". *Chem Lett*, 1992, 21: 1967–1970

11   Asato E, Katsura K, Mikuriya M, Turpeinen U, Mutikainen I, Reedijk J. Synthesis, structure, and spectroscopic properties of bismuth citrate compounds and the bismuth-containing ulcer-healing agent colloidal bismuth subcitrate (CBS). 4. crystal $(NH_4)_{12}[Bi_{12}O_8(cit)_8](H_2O)_{10}$. *Inorg Chem*, 1995, 34: 2447–2454

12   Asato E, Hol CM, Hulsbergen FB, Klooster NTM, Reedijk J. Synthesis, structure and spectroscopic properties of bismuth citrate compounds part II. Comparison between crystal structures of solid bismuth citrates and commercial CBS, using thermal and spectroscopic methods. *Inorg Chim Acta*, 1993, 214: 159–167

13   Herrmann WA, Herdtweck E, Pajdla L. "Colloidal bismuth subcitrate" (CBS): isolation and structural characterization of the active substance against *Helicobacter pylori*, a causal factor of gastric diseases. *Inorg Chem*, 1991, 30: 2579–2582

14   Li W, Jin L, Zhu N, Hou X, Deng F, Sun H. Structure of colloidal bismuth subcitrate (CBS) in dilute HCl: Unique assembly of bismuth citrate dinuclear units ($[Bi(cit)_2Bi]^{2-}$). *J Am Chem Soc*, 2003, 125: 12408–12409

15   Barrie PJ, Djuran MI, Mazid MA, McPartlin M, Sadler PJ, Scowen IJ, Sun H. Solid-state carbon-13 nuclear magnetic resonance investigations of bismuth citrate complexes and crystal structure of

Na$_2$[Bi$_2$(cit)$_2$]·7H$_2$O. *J Chem Soc Dalton Trans*, 1996, 2417–2422

16 Mayo SL, Olafson BD, Goddard III WA. Dreiding: a generic force field for molecular simulations. *J Phys Chem*, 1990, 94: 8897–8909 (b) Rappe AK, Casewit CJ, Colwell KS, Goddard III WA, Skiff WM. UFF, a full periodic table force field for molecular mechanics and molecular dynamics simulations. *J Am Chem Soc*, 1992, 114: 10024–10035 (c) *Cerius2* LigandFit, Accelrys Inc, San Diego, CA, 2003

17 (a) Burford N, Eelman MD, Mahony DE, Morash M. Definitive identification of cysteine and glutathione complexes of bismuth by mass spectrometry: assessing the biochemical fate of bismuth pharmaceutical agents. *Chem Commun*, 2003, 146–147 (b) Burford N, Eelman MD, Groom K. Identification of complexes containing glutathione with As(III), Sb(III), Cd(II), Hg(II), Tl(I), Pb(II) or Bi(III) by electrospray ionization mass spectrometry. *J Inorg Biochem*, 2005, 99: 1992–1997 (c) Phillips HA, Eelman MD, Burford N. Cooperative influence of thiolate ligands on the bio-relevant coordination chemistry of bismuth. *J Inorg Biochem*, 2007, 101:

736–739

18 Cole RB. *Electrospray Ionization Mass Spectrometry*. New York: Wiley, 1997

19 (a) Henderson W, Nicholson BK, McCaffrey LJ. Application of electrospray mass spectrometry inorganometallic chemistry. *Polyhedron*, 1998, 17: 4291–4313 (b) Colton R, D'Agostino A, Traeger J C. Electrospray mass spectrometry applied to inorganic and organometallic chemistry. *Mass Spectrom Rev*, 1995, 14: 79–106 (c) Cech NB, Enke CG. Practical implications of some recent studies in electrospray ionization fundamentals. *Mass Spectrom Rev*, 2001, 20: 362–387

20 Ferguson AD, Chakraborty R, Smith BS, Esser L, van der Helm D, Deisenhofer J. Structural basis of gating by the outer membrane transporter FecA. *Science*, 2002, 295: 1715–1719

21 Zhang L, Szeto KY, Wong WB, Loh TT, Sadler PJ, Sun H. Interaction of bismuth with human lactoferrin and recognition of the Bi^{III}-lactoferrin complex by intestinal cells. *Biochemistry*, 2001, 40: 13281–13287